Functionalized Nano Carbon for Excellent Microwave Absorption at GHz Frequency

Avanish Kumar Srivastava, Bhumika Samaria, Smita Soni, Anuj Shukla*, Umesh Kumar

Material Development Group, Defence Laboratory, Jodhpur 342011, India

*Corresponding author: E-mail: anuj.shukla@dl.drdo.in; avanish@dl.drdo.in; Tel: (+91) 2912511363; Fax: (+91) 2912510260

Received: 02 April 2019, Revised: 13 April 2019 and Accepted: 14 May 2019

DOI: 10.5185/amlett.2019.0027
www.vbripress.com/aml

Abstract

In the present study, nano carbon (NC) was chemically functionalized by refluxing in nitric acid for 6 h to form acid functionalized NC (FNC). TEM, XRD, FTIR, Raman, N_2 BET surface area and dc electrical conductivity characterizations confirm the functionalization and formation of surface oxygen functional groups, which in turn increase the hydrophilicity of FNC, thus rendering them solution processable. The basic framework of NC did not get change as confirmed from different characterization techniques. FNC were dispersed in an epoxy matrix by a solution blending method with different FNC loading levels (5, 7.0, 10, 12& 15 wt %). The FNC/epoxy composites were studied for electromagnetic properties in 8-12 GHz. Electromagnetic properties such as real and imaginary part of dielectric permittivity found increasing with increase of FNC loading. Reflection loss result of 10wt % of FNC composite shows RL >10 dB from 9.5 to12.0 GHz (absorption bandwidth~ 2.5 GHz) and effective absorption bandwidth (RL> 5dB) ~ 7 GHz (8-15 GHz). As a kind of potential microwave absorption material, the FNC composites are light weight and show excellent microwave absorbing ability.

Keywords: Nano carbon, composite, dielectric loss, microwave absorption, lightweight absorber.

Introduction

Microwave absorption materials have attracted a great deal of attention because of the rapid development in civil, commercial, military and airspace technology [**1-4**]. Hence, the situation demands an effective microwave absorbing materials which is able to control or reduce electromagnetic pollution and helps to increase the stealthiness of an Object by reducing its radar cross section [**5**]. Compared with conventional metal oxide, carbonaceous materials have more advantages in excellent corrosion resistance, light weight and low cost [**1**]. During the past few years, carbonaceous nanofillers such as carbon fibers, carbon nanotubes, carbon nanocoils and graphene have been considered as ideal substitute against metal oxide in electromagnetic pollution management [**6-15**]. For example, Song et al. reported 4.5 GHz of effective microwave absorption bandwidth with 5 wt% of porous carbon/ paraffin composite [**16**]. Al-Hartomy*et al.* reported dielectric and microwave properties of graphene nanoplatelets /carbon black filled natural rubber composites [**17**]. Savi *et al.* [**18**] analysed microwave absorption properties of epoxy filled with different concentration of multi walled carbon nano tubes. Wang et al reported dielectric and microwave attenuation properties of graphene nanoplatelet–epoxy composites [**19**]. Microwave absorption properties of nano carbon were also studied and reported [**20, 21**]. However, nano carbon, carbon fibers, carbon nanotubes and chemical vapour deposition graphene has predominant conductivity, thus their composites are mainly used for electromagnetic interference (EMI) shielding rather than absorption [**6, 22, 23**]. Moreover, reduced graphene oxide coupled with clustered defects as well functional groups and after modification using some macro- or nano-particles, has achieved promising microwave absorption performance [**24-25**].

Nano carbon black is a hydrophobic pigment which consists of 97–99% elemental carbon. In particular, NC with excellent electrical conductivity, low density, high corrosion resistance, excellent chemical stability, weather ability and colorability is considered as most promising application in paint industry, super capacitors, chemical sensors, and fuel cells etc., [**27-29**]. However, their hydrophobicity, self-aggregation and poor dispersion pose major challenges for their direct utilization via formation of NC filled composites or surface coatings. To overcome this, NC are often modified by covalent and non-covalent schemes (known as functionalization) which enhance their hydrophilicity, process ability and compatibility [**30-34**]. It is worth mentioning that functionalized NC contain polar groups which enable their dispersion inside solvents, enhances compatibility with polymeric

matrices and improves their ability to surface coat the polymeric substrate based packaging materials [**35, 36**]. One of the ways to functionalize NC is to oxidize the surface of NC by acid treatment to get its hydrophilic nature via introducing surface oxygen functional groups.

In this study, we successfully synthesized functionalized NC by refluxing NC in nitric acid which was dispersed in an epoxy medium by a solution blending method. The corresponding epoxy nanocomposites with different FNC loading levels were studied for the electromagnetic and microwave absorption properties. For the fundamental research, it is worth to study new and unexplored composite systems for their physical properties, including dielectric and microwave attenuation properties, which can broaden further research on this subject and becomes our major motivation and incentive for this work.

Experimental

Materials

Nanocarbon (Ketzen black 600 purchased from Akzo Nobel, Netharlands), nitric acid (assay, 70%, purchased from Merck, India). Epoxy resin (M/s Synpol Products Pvt. Ltd., India) was used as matrix for composite preparation.

Functionalization of nanocarbon

About 50 g of pristine NC was dispersed in 500 mL distilled water containing 10 wt % nitric acid by ultra-sonication for 2h followed by refluxing the mixture at 90ºC for 6 hrs. This was further followed by filtration using a vacuum filtration assembly. The sample was repeatedly washed with distilled water till neutral pH of filtrate. The filtered FNC was dried in an oven at 110ºC for 12 h.

Preparation of FNC /epoxy composite

The FNC at different loading levels (5.0, 7.0, 10.0, 12.0, 15.0 wt %) was dispersed into epoxy resin and the mixture was blended at 500 rpm for 15 min by a shear mixer (overhead stirrer, IKA) to make a homogeneous blend, thereafter, a curing agent was further added into the blend and mix it further for 10 min. Finally, the mixture was poured into the mold and cured at room temperature for 6 h. After curing, composite sheet was carefully removed from the mould. The FNC/epoxy composites were then used for measurement of electromagnetic and microwave absorption properties.

Characterizations

Transmission electron microscopy (TEM, Tecnai F30 G2, FEI, USA)) was used to analyze the surface morphology and particle size. The atomic force microscope (Solver Pro, 2007) was employed to evaluate the morphology and estimation of particle size of FNC.The Fourier transform infrared (FTIR) spectra were recorded in KBr with a resolution of 2 cm^{-1} and scan range of 400-4000 cm^{-1} by using ATR-FTIR spectrophotometer, Agilent; Model: 660. Pellets were formed after pressing in hydraulic press at about 1.5 tonne/cm^2 for the FTIR measurements. Raman spectra of the powder samples were recorded on an Avalon Raman microscope R3-532 using aTEGOn ion laser (λ= 532 nm) in the range of 1000–2000 cm^{-1}.The structural characterization of the samples was carried out by the powder X-ray diffractometer (Philips X'PertPro diffractometer) using CuKα (λ = 0.154 nm) radiation source operated at the voltage of 40kV and current of 30mA over the scattering angle ranging from 2Θ=10-60^0 with a step size of 0.05^0/min. N_2 adsorption isotherms were measured at 77 K on a Micromeritics, ASAP-2020. The specific surface area was calculated from the Brunauer-Emmett-Teller method (BET). DC electrical conductivity of these materials was measured at room temperature by Hall Effect method using Hall Effect measurement system, model HMS-3000.Vector network analyzer (VNA, model Hewlett-Packard 8510) was used to obtain S-parameters of the samples in the 8-12 GHz range at room temperature. For wave guide measurements composites were cut in rectangular shape (length: 22.8 mm, width: 10.1mm and thickness: 2.0 mm) and inserted in the waveguide. EM parameters (complex permittivity and complex permeability) of the FNC/epoxy composites were calculated from the measured values of S-parameters using Nicolson-Ross algorithm [**36**]. The microwave absorbing properties of a one-layer absorber backed by a metallic plate were measured in anechoic chamber as well as investigated by means of numerical simulations considering a plane wave incidence on the dielectric stratification and a transmission line approach [**37**].

Results and discussion

Physiochemical characterization

Fig. 1(a) and **Fig. 1(b)** show the actual refluxing setup used to carry out the reaction and dispersed FNC in ethanol.

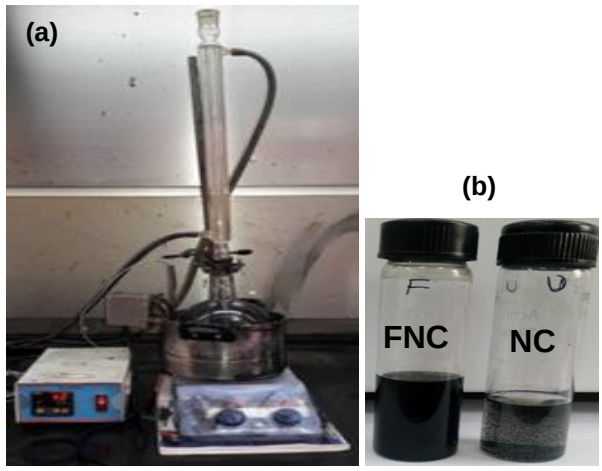

Fig. 1. (a) Actual refluxing setup and (b) dispersion images of FNC.

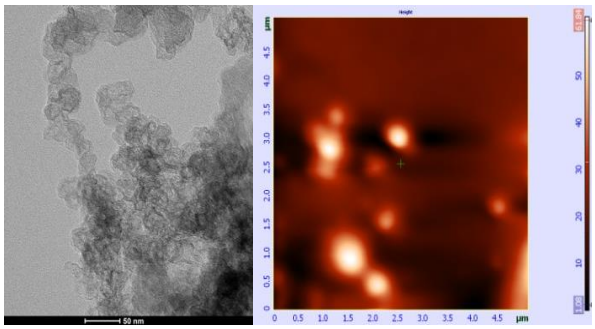

(a) (b)

Fig. 2. (a) TEM images (b) AFM images of FNC.

As shown in typical TEM images **(Fig. 2a)**, FNC were found spherical in shape with diameter less than 50 nm and most of the particles are severely aggregated due to the high surface energy. The morphology of the FNC remained unaltered even after harsh acid treatment. AFM imaging results **(Fig. 2b)** further confirm the spherical shape with diameter 25-30 nm. FTIR spectra of FNC (**Fig. 3a**) shows peak at ~ 1585 cm^{-1} in both samples due to the stretching vibrations of the -C=C- bond which constitute the NC backbone. The presence of this peak in both NC and FNC shows that the basic skeleton of NC is preserved even after the acid treatment. However, the appearance of additional peaks corresponding to O–H stretching vibration of absorbed water molecules (3403 cm^{-1}), C=O (1718 cm^{-1}), carboxy C–O (1384 cm^{-1}), C–O of epoxy (1260 cm^{-1}) and C–O of alkoxy groups (1074 cm^{-1}) and reduction in relative intensity of –C=C– stretch peak in FNC confirms the successful oxidation of NC. These peaks are either weak or absent in pristine NC [**37**]. These results are complimented by the Raman spectra (**Fig. 3b**) which shows that the intensity of D-band relative to G-band (i.e. I_D/I_G ratio) is higher for FNC as compared to pristine NC. This indicates that a sufficiently large number of defects have been created upon functionalization which can serve as functional handle and active surface sites for the dispersion of FNC (Fig. 1b) inside polar solvents (e.g. ethanol in present case) & their interaction with epoxy matrix as well. XRD of NC and FNC (**Fig. 3c**) displayed broad diffraction peaks at 2θ=25.2°and 42.1° and 49.2° attributed to the coke-like structure planes {002}, {100} and {004} respectively. Broaden peak at 25.2° indicate disordered carbonaceous interlayer [**37**]. Further, the absence of any new peak in Raman and XRD spectra and only minimal shift in peak position (**Fig. 3b &c**) revealed that the basic structure of NC remained unaffected by functionalization. The N_2 BET surface area of NC and FNC werefound 1315 m^2/g,1180 m^2/g and pore volume 2.61 g/cc, 2.42 g/cc respectively. The decrease in N_2 BET surface area and pore volume of NC was due to the conversion of few micropores to mesopores (**Fig. 3d**). The pore diameter of NC (65A^0) remained unaffected after functionalization (65A^0). Room temperature dc electrical conductivity values (σ) of NC and FNC was found to be 5.0 and 0.4 S/cm respectively.Conductivity of FNC was found lesser than NC due to disruption in SP^2 symmetry with the incorporation of oxygen functional groups as evidenced in Raman and FTIR spectra.

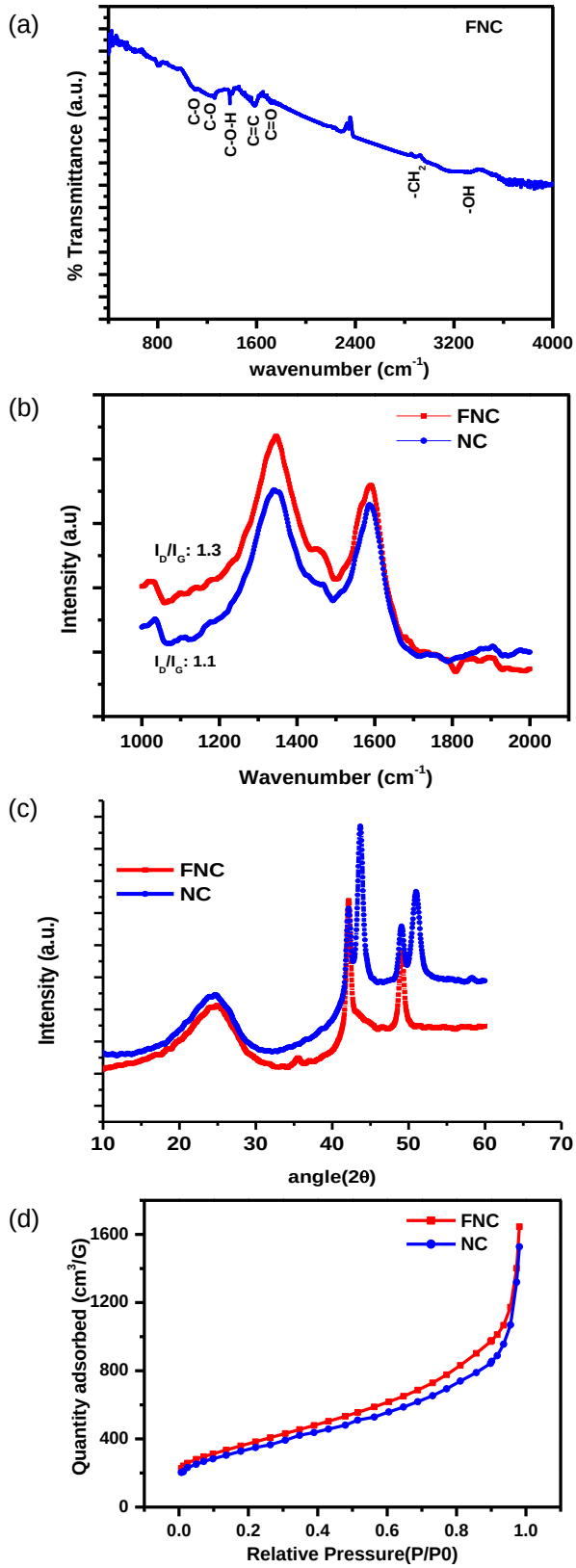

Fig. 3. (a) FTIR spectra (b) Raman spectra (c) XRD Spectra (d) Adsorption isotherm of NC and FNC.

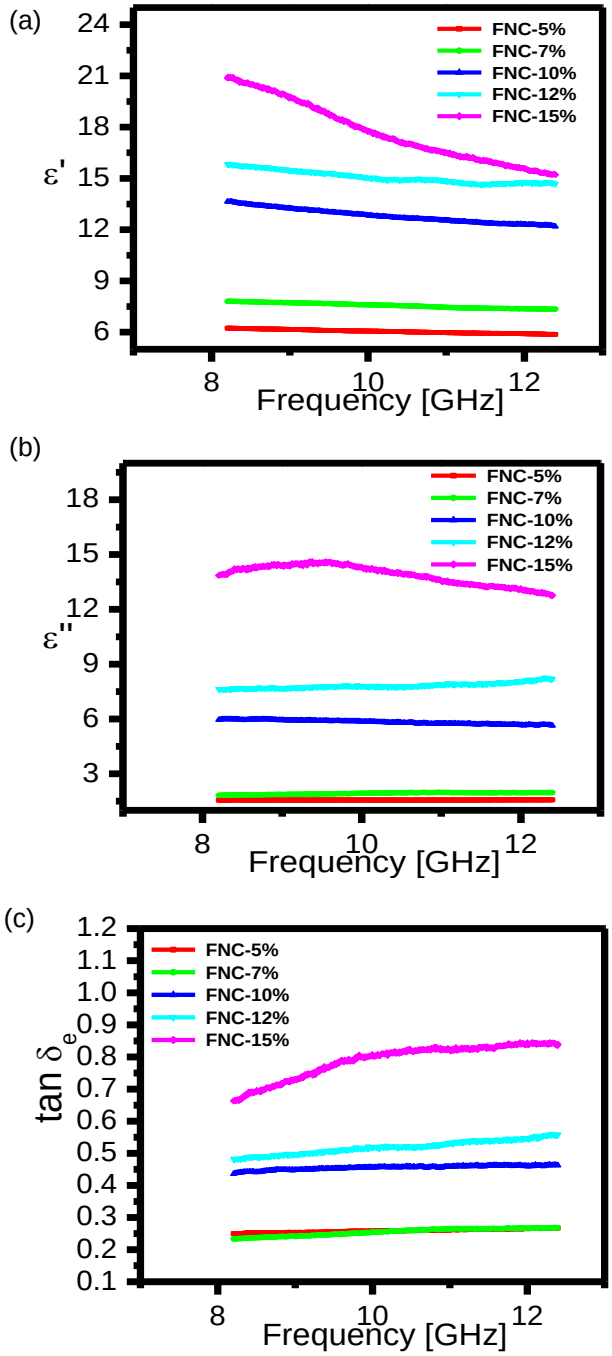

Fig. 4. Frequency dependence on (a) real part of complex permittivity, (b) imaginary part of complex permittivity (c) dielectric tangent loss of FNC composites (5-15 wt %).

Microwave absorption properties

The MA of composites was calculated using measured complex permittivity, ε_r by means of numerical simulations [**38**]. **Fig. 4a** and **Fig. 4b** shows the measured ε' (real part) and ε'' (imaginary part) values of ε_r in the range of 8–12 GHz for the composites containing 5.0, 7.0, 10.0, 12.0 and 15.0 wt % FNC. The ε' values increase with increase of the FNC concentration and it can be attributed to the increment of dipolar polarization and electrical conductivity [**10, 26**]. The decrease of ε' with the increase of frequency may arise from the lags of induced charges in the material to follow the reversing electromagnetic field in the high frequency range. ε'' represents how dissipative a material is to external electromagnetic field. So ε'' is directly related to the microwave absorption of the material. ε'' values of composites increases from 1.55 to 13.85 with the increase of filler loading from 5-15 wt %. The increase in ε' and ε'' with the increase in concentration of nanocarbon is in agreement with the findings of Adohi *et al.* **[26]**. Our FNC based composites show better dielectric permittivity as reported by Brosseau et al where ε' and ε'' found in the range of 6-4 and 0.4-0.5.for carbon black -epoxy composite containing 7 vol % over the frequency range 1–10 GHz [**39**]. Dielectric loss tangent (tan $\delta = \varepsilon''/\varepsilon'$) was compared, which is related to microwave attenuation in dielectric materials, and **Fig. 4c** shows the tanδ of each sample. All composite samples showed $\mu_r = 1$ in 8–12 GHz. implying that the microwave absorption of FNC composites was mainly attributed to the dielectric loss.

The return loss (RL) curves of a metal-backed single absorbing layer were calculated in the frequency range of 8–18 GHz according to the transmission line theory. It can be expressed as the following equation: [**40**]

$$RL\ (dB) = 20 \log \left| (Z_{in}-1)/(Z_{in}+1) \right| \quad (A1)$$

$$Z_{in} = (\mu_r/\varepsilon_r)^{1/2} \tanh [(j2\pi fd/c)\ (\mu_r\varepsilon_r)^{1/2}] \quad (A2)$$

where Z_{in} is the characteristic input impedance of the absorber, f is the frequency of microwaves, d is the thickness of the absorber, and c is the velocity of microwave in free space. According to Eqs. (A1) and (A2), the RL of the absorbing material is a function of six parameters: ε', ε'', μ', μ'', f, dand c. For the given EM parameters, the RL of composites with different thicknesses at each frequency can be calculated according to Eqs. (A1) and (A2). In general, materials with RL > 10 dB (90% absorption) are considered as efficient microwave absorbers.

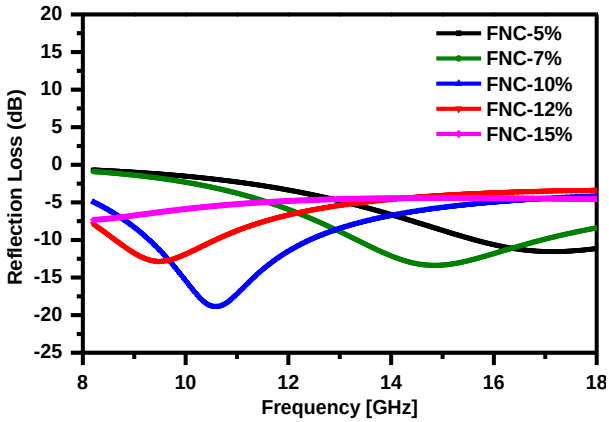

Fig. 5. Calculated electromagnetic RL of FNC composites (5-15 wt %) with 2.0 mm thickness.

The simulated RL of composites containing different filler loading (5.0, 7.0, 10.0, 12.0 and 15 wt %) at 2.0 mm thickness are shown in **Fig. 5**. Composite with 10 wt % loading was found to produce highest effective MA bandwidth (RL> 10dB) ~ 3.1 GHz (9.3-12.4 GHz) and (RL> 5dB) ~ 8 GHz (8-16 GHz) and maximum RL (RL_{max}) 19dB at 10.5 GHz. Moreover, the absorption frequency ranges can be shifted by changing the wt.% of FNC even while keeping the thicknessconstant at 2 mm. Similar results has been observed by Gogoi *et al.* in exfoliated graphite- novolac phenolic resin. Absorption bandwidth of 0.8 GHz (9.3–10.1 GHz) could be achieved with 10 wt % exfoliated graphite [**41**]. Multi walled carbon nanotube (MWCNT) –epoxy composites prepared by Savi et al using5wt % of MWCNT showRL >10 dB in 7.2-9.3 GHz (effective absorption bandwidth~ 2.1 GHz) [**18**]. The simulated RL for 12 wt % composite shows effective MA bandwidth ~ 1.8 GHz (8.7-10.5 GHz) and RL_{max} 13dB at 9.6 GHz. The effect of thickness on MA has also been studied for the composite with 10 wt % loading and results are presented in **Fig. 6**. As evidenced from the figure the values of maximum RL (RL_{max}) increases slightly with shifting to lower frequency region and effective MA (RL>10dB) bandwidth decreases with the increase of thickness. Peak shifting with thickness change could be explained by quarter wavelength attenuation phenomenonwhich states that the electric filed is maximum at the λ/4 distance from metal ground and decreases along with the incident the propagating direction of the incident electromagnetic wave [**18, 42**]. According to the loss mechanism of the λ/4 resonance, when the thickness of a material is around λ/4, the reflected waves will superpose with each other to form a destructive interference. In an ideal case, the reflected waves are completely cancelled.

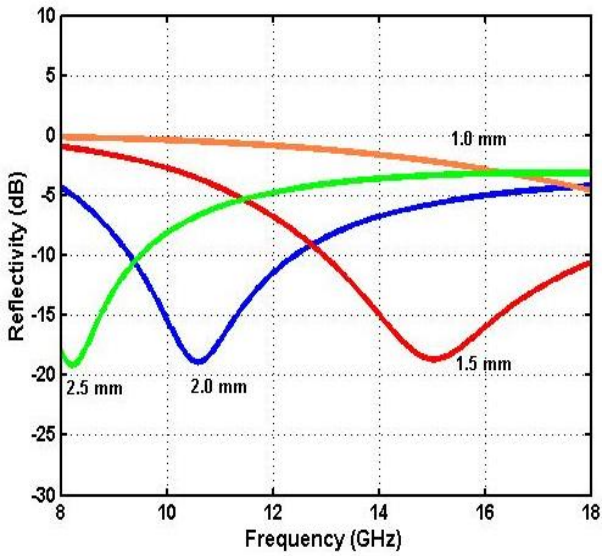

Fig. 6. Calculated RL of FNC composites (10 wt %) with different thickness ranging from1.0-2.5 mm.

Furthermore, in order to evaluate the real MA performance, FNC/epoxy composites 80 mm (l) × 80 mm (w) x 2.0 mm (t) were prepared with 10 and 12wt % of FNC. The composites were backed by aluminum plate and RL measured in anechoic chamber. The Measured RL >10 dB from 9.5 to12.0 GHz (MA bandwidth~ 2.5 GHz) and effective MA bandwidth (RL> 5dB) ~ 7 GHz (8-15 GHz) was found for 10wt % of FNC composite. FNC composite with12wt % loading show effective MA bandwidth (RL>10dB) ~ 1.8 GHz (8.7-10.5 GHz). The RL_{max} for 10 and 12 wt % of FNC composite was found 15 and 13 dB at 10.5 and 9.6 GHz respectively. The measured RL of composites (**Fig. 7**) were found closer to simulated RL as evident from **Fig. 5** and slight variation in effective MA bandwidth may be attributed to sample preparation.

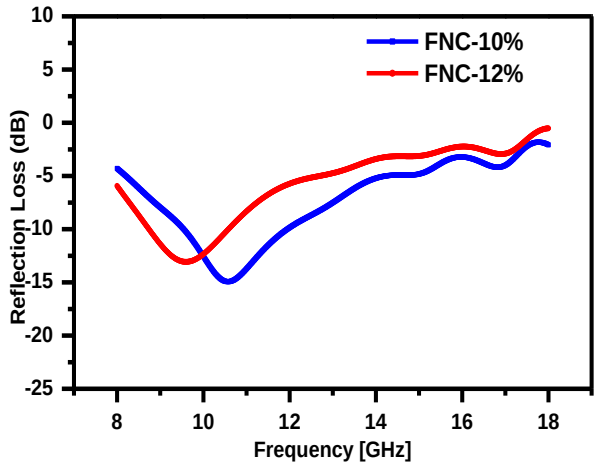

Fig. 7. Measured RL of FNC composites (10 and 12 wt %) with 2.0 mm thickness.

Conclusion

The NC was successfully functionalized by refluxing in nitric acid which results into improved dispersion into epoxy matrix. Characterization results shows retention of the basic framework of NC even after acid treatment. The EM and MA studies of FNC/epoxy composites show good MA properties with 10 wt % filler loading. The effective MA bandwidth is 2.5 GHz (from 9.3 to 12.4 GHz) and the maximum RL can reach up to 15 dB at 10.5 GHz for FNC composite with 10 wt % loading. NC carbon being commercially available with low cost can be used as an alternative to costly graphene and carbon nanotubes for MA applications after functionalization which results into improved dispersion and MA.

Acknowledgements

The authors are thankful to Shri Ravindra Kumar, Director Defence Lab for his inspiration and valuable guidance. We are also thankful to Anjali Bhatia for their kind support and useful suggestions. We are thankful to Yojana Janu, Amit Sadh, Rajesh Nunia, Manjeet Kulhar and G. K. Prasad for carrying out XRD, Raman, FTIR, electrical conductivity and surface area measurements respectively.

References

1. Xianguo, L.; Caiyun, C.; Jieyi, Y.; Sun, Y.; Xia, Ailin.; *Mater. Lett*., **2018**, *225*, 1.
2. Lv, H. L.; Yang, Z. H.; Wang, P. L.; Ji, J.; Song, J.; Zheng, L.; Zeng, H.; Xu. J, Z.; *Adv. Mater*., **2018**, *30*, 1706343.
3. Kuang, B.; Song, Weili.; Ning, M.; Li, Jingbo.; Zhao, Z.; Guo, Deyu.; Cao, M.; Jin, H.; *Carbon*, **2018**, *127*, 209.
4. Cao, Y.; Ai, S. G.; Zhang, J.; Gu, Ning.; Hu, S.; *Adv. Mat. Lett*., **2013**, *4*, 160.
5. Li, G.; Xie, T.; Yang, S.; Jin, J.; Jiang, J.; *J. Phys. Chem. C*., **2012**, *116*, 9196.
6. Chen, Z.; Xu, C.; Ma, C.; Ren, W.; Cheng, H.; *Adv. Mater*, **2013**, *25*, 1296.
7. Zhang, X. J.; Wang, G. S.; Cao, W. Q.; Wei, Y. Z; Cao, M. S.; Guo, L.; *RSC Adv*., **2014**, *4*, 19594.
8. Chen, X.; Meng, F.; Zhou, Z.; Tian, X.; Shan, L.; Zhu, S.; Xu, X.; Jiang, M.; Wang, L.; Hui, D.; Wang, Y.; Lu, J.; Gou, J.; *Nanoscale*., **2014**, *6*, 8140.
9. Wu, F.;Wang, Y.; Wang, M. Y.; *RSC Adv.*, **2014**, *4*, 49780.
10. Kong, L.; Yin, X. W.; Yuan, X. Y.; Zhang, Y. J.; Liu, X. M.; Cheng L. F.; Zhang, L. T.; *Carbon*, **2014**, *73*, 185.
11. Sun, D.; Zou, Q.; Wang, Y.; Wang, Y.; Jiang, W.; Li, F.; *Nanoscale*., **2014**, *6*, 6557.
12. Ren, Y.; Zhu, C.; Zhang, S.; Li, C.; Chen, Y.; Gao, P.; Yang, P.; Ouyang, Q. Y.; *Nanoscale*, **2013**, *5*, 12296.
13. Ren, Y. L.; Wu, H. Y.; Lu, M. M.; Chen, Y. J.; Zhu, C. L.; Peng, G.; Cao, M. S., Li, C. Y.; Ouyang, Q. Y.; *ACS Appl. Mater. Interfaces*, **2012**, *4*, 6436.
14. Wang, G.; Gao, Z.; Tang, S.; Chen, C.; Duan. F.; Zhao, S.; Lin, S.; Feng, Y.; Zhou, L.; Qin, Y.; *ACS Nano*, **2012**, *6*, 11009.
15. Wang,G.; Gao, Z.; Wan, G.; Lin, S.; Yang, P.; Qin, Y.; *Nano Res*., **2014**, *7*, 704.
16. Song, W. L.; Cao, M. S.; Fan, L. Z.; Lu, M. M.; Li, Y.; Wang, C. Y.; Ju, H. J.; *Carbon*, **2014**, *77*, 130.
17. Omar, A.; Al, H. A.; Al-Ghamdi, F.; Al-Salamy, N. D., Shtarkova, R.; Iliev V.; El-Tantawy, F.; *International Journal of Mat. and Chem*., **2012**, *2*, 116
18. Savi, P.; Miscuglio, M.; Giorcelli, M.; Tagliaferro, A.; *Prog. In Electromagnetics Research Letters*, **2014**, *44*, 63.
19. Wang, Z.; Luo, J.; Zhao, G. L.; *AIP Advances*,**2014**, *4*, 017139.
20. Fiorellino, F.; Pilloni, M.; Ardu, A.; Cabras, V.; Columbu, S.; Russo, L.; Scano,A.; Ennas, G.; *Adv. Mat. Lett*., **2019**, *10*, 253.
21. Chung, K. T.; Sabo, A.; Pica, A. P.; *J. Appl. Phys*.; **1982**, *53*, 6867.
22. Yang, Y.; Gupta, M.; Dudley, K. L.; Lawrence, R. W.; *Nano Lett*., **2005**, *5*, 2131.
23. Tiwari, A.; *Adv. Mat. Lett*., **2012**, *3*, 172
24. Chaturvedi, A.; Tiwari, A.; Tiwari, A.; *Adv. Mat. Lett*., **2013**, *4*, 656.
25. Srivastava, A. K.; Samaria, B.; Soni, S.; Chauhan, V.S.; Singh, Jitendra.; Shukla, R. K.; Shukla, A.; Kumar N.; *Adv. Mat. Procd*., **2018**, *3*, 85.
26. Adohi, B. J.P.;Mdarhri, A.;Prunier, C.; Haidar, B.; Brosseau, C.; *J. Appl. Phys.*, **2010**, *108*, *074108*.
27. Qin, H.; Liao, Q.; Zhang, G.; Huang, Y.; Zhang, Y.; *Appl. Surf. Sci*., **2013**, *286*, 7.
28. Atif, M.; Bongiovanni, R.; Giorcelli, M.; Celasco, E.; Tagliaferro, A.; *Appl. Surf. Sci.*, **2013**, *286*, 142.
29. Jiang, K.; Fei, T.; Jiang, F.; Wang, G.; Zhang, T.; *Sensors and Actuators B*, **2014**, *192*, 658.
30. Chen, J.; Hamon, M. A.; Hu, H.; Chen, Y.; Rao, A. M.; Eklund, P. C.; Haddon, R. C.; *Science*, **1998**, *282*, 95.
31. Bianco, A.; Kostarelos, K.; Partidos, CD.; Prato, M.; *ChemCommun*., **2005**, 571.
32. Che, R.; Peng, L. M.; Duan, X. F.; Chen, Q.;, Liang, X. L.; *Adv. Mater*., **2004**, *16*, 401.
33. Fu, S.; Du, C.; Wang, C.; Tian, A.; Xu, *Colloids and Surfaces A: Physicochemical. Eng. Aspects*, **2013**, *428*, 1.
34. Shi, P. W.; Li, Q. Y.; Li, C. Y.; Wu, C. F.; *Colloids and Surfaces A: Physicochem. Eng. Aspects*, **2014**, *443*,135.
35. Song, Y. S.; Youn, J. R.; *Carbon*, **2005**, *43*, 1378.
36. Nicolson, A.M.; Ross, G.F.; IEEE Trans. on Instrumentation and Measurements, **1970**, *4*, 377.
37. Khan, W.; Sharma, R.; Chaudhury, P. K.; Siddiqui, A. M.; Saini, P.; *Int J. Nanomater. Nanotechnol. Nanomed*., **2016**, *2*, 025.
38. Savi, P.; Trinchero, D.; Tascone, R.; Orta, R.; IEEE Trans. on Microwave Theory and Techniques., **1997**, *45*, 221.
39. Brosseau, C.; Boulic, F.; Queffelec, P.; Bourbigot, C.; Mest, Y. L.; Loaec, J.; Beroual, A.; *J. Appl. Phys.*, **1997**, *81*, *882.*
40. Qin, F.; Brosseau, C.; *J. Appl. Phys.*, **2012**, *111*, 061301.
41. Gogoi, J.P.; Saxena, N.; Bhattacharyya, Satyaji; *Composites: Part B*, **2014**, *58*, 518
42. Song, W. L.; Cao, M. S.; Wen, B.; Hou, Z. L.; Cheng J.; Yuan, J.; *Mater. Res. Bull.*, **2012**, *47*, 1747.

